Sociedad Geológica de España

GEOGACETA, 76, 2024

δ^{13}C and δ^{18}O-based interpretation of Miocene carbonates of the Miranda-Trebiño basin, NE Iberia: preliminary insights

Interpretación basada en δ^{13}C y δ^{18}O de los carbonatos del Mioceno de la cuenca de Miranda-Trebiño, NE Iberia: primeros resultados

Zuriñe Larena[1*], Concha Arenas[2, 3], Xabier Murelaga[1] and Juan Ignacio Baceta[1]

[1] Departamento de Geología, Facultad de Ciencia y Tecnología. Euskal Herriko Unibertsitatea UPV/EHU Apartado 644, E-48080 Bilbao. zurine.larena@ehu.eus, juanignacio.baceta@ehu.eus and xabier.murelaga@ehu.eus
[2] Departamento de Ciencias de la Tierra, Universidad de Zaragoza, Pedro Cerbuna 12, E-50009-Zaragoza. carenas@unizar.es
[3]Institute for Research on Environmental Sciences of Aragón (IUCA) and GeoTransfer Group.
*Corresponding autor

ABSTRACT

The stable isotopes (C and O), bulk mineralogy and sedimentary facies types of the Miocene lacustrine-palustrine carbonates of the Cucho Section (Miranda-Trebiño basin, N Iberia) are studied. The results indicate deposition in a freshwater carbonate lake recording significant biogenic CO_2 input, changing Precipitation/Evaporation rates and variations in vegetation cover and pedogenesis on palustrine areas. Short-lived stages of higher salinity and evaporative conditions are recorded by the relative abundance of fine-grained dolomite. The highest δ^{13}C values suggest ^{12}C sequestration in anoxic bottom waters due to water column stratification. These new data support the general deepening trend of the lake system established from previous sedimentological analyses.

Key-words: *Lacustrine-palustrine, carbonates, δ13C, δ18O, Climate, Hydrology.*

RESUMEN

Se presenta el estudio integrado de facies sedimentarias, isótopos estables (C y O) y mineralogía total de los carbonatos miocenos lacustres-palustres de Cucho (Cuenca de Miranda-Trebiño, Norte de Iberia). Los resultados indican un contexto de lago carbonatado de agua dulce que registró aporte significativo de CO_2 biogénico, cambios en la relación Precipitación/Evaporación y variaciones en la cobertera vegetal y pedogénesis en contextos palustres. Se infieren estadios de elevada salinidad y evaporación a partir de la abundancia relativa de dolomita de grano fino. Los valores más altos de δ^{13}C podrían asociarse al secuestro de ^{12}C en el fondo anóxico por estratificación de la columna de agua. Los datos apoyan la tendencia de profundización general deducida por análisis sedimentológicos previos.

Palabras clave: *Lacustre-palustre, carbonatos, δ13C, δ18O, clima, hidrología.*

Geogaceta, 76 (2024), 19-22
https://doi.org/10.55407/geogaceta104481
ISSN (versión impresa): 0213-683X
ISSN (Internet): 2173-6545

Fecha de recepción: 09/02/2024
Fecha de revisión: 19/04/2024
Fecha de aceptación: 07/06/2024

Introduction

The environmental information (i.e., depositional, climatic and hydrologic conditions) obtained from stratigraphic and sedimentologic studies of lacustrine and palustrine carbonate systems can be complemented with geochemical proxies, such as δ^{13}C and δ^{18}O (Talbot and Kelts, 1990; Benavente et al., 2019). In addition, mineralogical and paleontological proxies also provide useful data for environmental interpretation (Moreau et al., 2023). In the Iberian Peninsula, such multidisciplinary approach has been applied with success to the Oligocene and Miocene successions of the Ebro, Duero and Madrid basins (Alonso-Zarza et al., 1992; Arenas et al., 1997; Luzón et al., 2002; Armenteros et al., 2002). However, many other, usually smaller, continental basins in Iberia still lack such type of multidisciplinar database.

This work presents the first δ^{13}C and δ^{18}O data from the Lower Miocene palustrine and lacustrine deposits exposed in the Cucho section (Miranda-Trebiño Basin, MTB; Fig. 1). These preliminary results complement previous stratigraphic and sedimentologic information of the same section (Larena et al., 2024) by giving further evidence of environmental conditions during the deposition of those carbonates.

Geological setting. Stratigraphic and sedimentologic context

The study area is located in the MTB, a piggy-back basin developed in the southern sector of the Basque-Cantabrian Pyrenean region during the emplacement of the Sierra de Cantabria-Montes Obarenes thrust sheet over the Ebro and Duero foreland basins. It developed from the late Paleogene until the Middle Miocene. The MTB contains up to 3000 m of continental deposits (clastic and carbonate) representing different depositional conditions, from alluvial to palustrine-lacustrine environments (Riba, 1956, 1961; Riba and Jurado, 1992).

The succession studied at Cucho consists of 160 m of carbonate (limestones, and rare dolomitic limestones and dolostones), clastic (mudstones and sandstones), mixed (marls and marlstones), and organic-rich facies (coal layers) (Larena et al., 2024). These facies are grouped into three facies associations representing alluvial (FA1), palustrine (FA2) and lacustrine (FA3) environments. This work is focused on the carbonate facies of FA2 and FA3. Bioturbated massive wackestones (Lwb) and nodular marly limestones (Lwn) are representative facies of FA2.

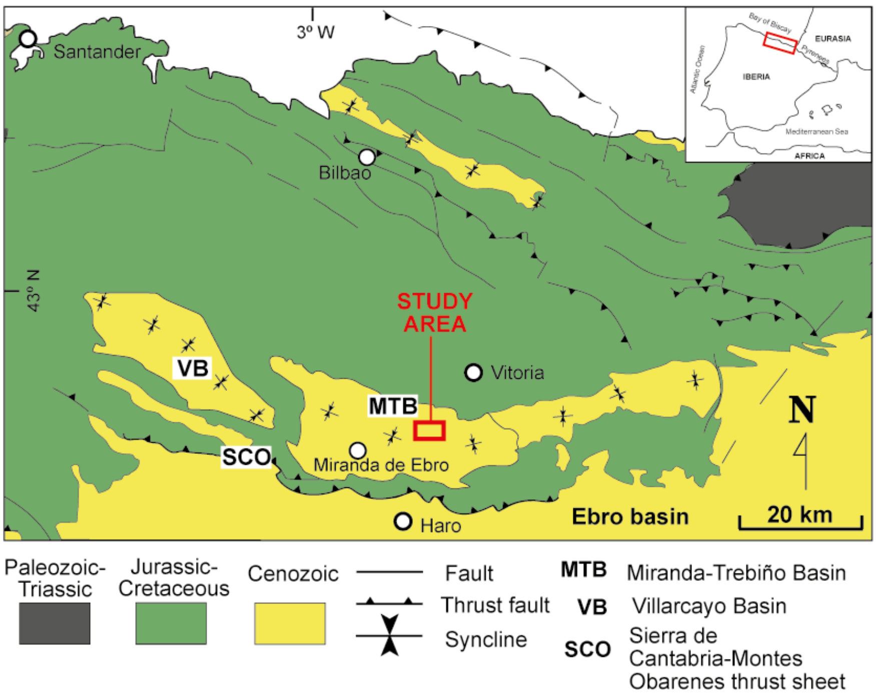

Fig. 1.- Location of the Cucho section in the Basque-Cantabrian Pyrenean Basin and in the Miranda-Trebiño Basin (MTB). See the color figure in the Web.

Fig. 1.- Localización de la sección de Cucho en la Cuenca Vasco-Cantábrica pirenaica y la Cuenca de Miranda-Trebiño. Ver figura en color en la Web.

Massive wackestones (Lwm), mudstones with scattered silt-sized quartz grains (Lmq), laminated wackestone-packstones (Lw-pl), laminated mudstone-wackestone (Lw-wl) and massive dolostones (MD) characterise FA3.

Five stratigraphic sequences, 28 to 43 m thick, have been described in the Cucho section (S1 to S5; Fig. 2). Their boundaries are abrupt facies changes. The sequences represent five asymmetric depositional cycles, each starting with terrigenous fluvial facies grading vertically to palustrine and lacustrine fine-grained carbonate deposits (Larena et al., 2024). The cycle trends are finning-upward, but the general trend of the Cucho succession exhibits a coarsening-upward evolution up to the base of cycle S4, given by the increasing thickness and grain size of the detrital deposits in S4, and afterward a gentle fining-upward evolution.

Methodology

Thirty samples corresponding to the different carbonate facies mentioned above were selected through the Cucho section (Table I; Fig. 2) for mineralogical and stable isotope ($\delta^{13}C$ and $\delta^{18}O$) analyses. Prior to sampling, all carbonate samples were texturally characterised through petrographic observations. Then, samples for the geochemical analyses were obtained with a microdrill, avoiding cements and other artifacts (e.g., fossils or organic matter).

The mineralogical composition of all samples was determined by X-ray diffraction. The analyses were carried out at the X-Ray Services, Unit of Rocks and Minerals of the General Research Services (SGIker) of the University of the Basque Country (Spain), using a PANalytical CubiX diffractometer, equipped with copper tube, vertical goniometer, programmable slits, automatic sample exchanger, filter nickel and PixCel detector. The measurement conditions have been 40 KV and 40 mA, with a sweep between 5 and 70° 2 theta.

Sample	Facies	% Calcite	% Dol	% Quartz	% Arg	$\delta^{13}C$ (‰VPDB)	$\delta^{18}O$ (‰VPDB)	Sample	Facies	% Calcite	% Dol	% Quartz	$\delta^{13}C$ (‰VPDB)	$\delta^{18}O$ (‰VPDB)
C1-1	Lmq	93	1	6		-1.7	-7.24	**C3-2**	Lwm	92	1	7	-1.7	-5.57
C1-5	MD		99	1		-1.7	-0.83	**C3-6**	Lwm	98		2	-1.65	-5.88
C1-7	Lm-wl	72		28		-5.17	-3.36	**C3-8**	Lwm	98		2	0.58	-6.2
C1-8	MD		98	2		-2.88	-0.79	**C3-9**	Lw-pl	98		2	0.76	-5.55
C1-9	Lwb	95		5		-2.9	-5.92	**C3-11**	Lwm	100			-0.81	-6.11
C1-12B	Lm-wl	94	2	4		-5.33	-5.63	**C3-15**	Lwm	98		2	-5.24	-5.62
C1-14	Lm-wl	80	18	2		-3.16	-5.64	**C3-16**	Lwm	100			-6.74	-7.9
C2-3	Lwn	98		2		-3.97	-6.65	**C3-18**	MD	40	59	1	-5.22	-1.86
C2-5	Lwn	95		5		-6.28	-6.94	**C3-23**	Lwm	100	1		1.04	-5.59
C2-6	Lmq	79	6	15		-5.88	-7.37	**C3-25**	Lwm	99		1	0.01	-4.53
C2-8	MD		85	15		-4.63	-1.73	**C3-29**	Lwm	98		2	-1.58	-5.57
C2-13	MD		96	4		-4.24	-1.24	**C3-31**	Lw-pl	99		1	-0.5	-6.01
C2-14	MD		98	2		-4.51	-1.77	**C4-1B**	Lw-pl	97		3	3.01	-5.8
C2-19B	Lw-pl	87		5	8	-1.37	-4.86	**C4-2A**	Lw-pl	99		1	2.33	-4.3
C2-21*	Lw-pl	92		8		-0.65	-3.05	**C4-3**	Lw-pl	96		4	0.06	-5.91

Table I.- Mineralogical and $\delta^{13}C$ and $\delta^{18}O$ data. Sample C2-21* contains traces of smectite. The mineral composition is indicated in % weight as semiquantitative estimation. Location of samples is in Figure 2. Dol: dolomite. Arg: aragonite.

Tabla I.- Datos de mineralogía, y valores de $\delta^{13}C$ y $\delta^{18}O$. La muestra C2-21 contiene indicios de esmectita. La composición mineral se indica en % en peso como estimación semicuantitativa. Localización de las muestras en la Figura 2. Dol: dolomita. Arg: aragonito.*

The $\delta^{13}C$ and $\delta^{18}O$ ratios were performed at the Servicios Científico-Técnicos of the University of Barcelona. The values were measured in a mass spectrometer (MAT-252, Thermo Finnigan; Thermo Fisher Scientific, Waltham, MA, USA), following standard procedures (McCrea, 1950). The results are reported in δ‰ notation relative to Vienna Pee Dee Belemnite (VPDB). The reproducibility was better than ±0.03 in $\delta^{13}C$ and ±0.06 in $\delta^{18}O$.

Results

Bulk mineralogy

Table I shows the mineralogical composition of all analysed carbonate samples. Most samples are formed of calcite, with values ranging between 72 to 100% of the bulk rock. In most of the samples there are very small amounts of detrital quartz (0 to 8%), except for three samples that contain between 15 and 28%.

A few samples have high dolomite content (Fig. 2): one in S1, one in S2, three in S3 and one in S5. Quartz content varies between 0 and 28%. Clay minerals are rare to absent; only smectite has been identified in one sample from the base of the section (C2-21).

$\delta^{18}O$ and $\delta^{13}C$ data

Table I shows the $\delta^{13}C$ and $\delta^{18}O$ values of the analysed samples, whose temporal distribution is in Figure 2.

The set of values has wide variability: $\delta^{18}O$ values vary between -0.79 and -7.9 ‰ (mean: -4.85±2.04 ‰) and $\delta^{13}C$ between 3.01 and –6.74 ‰ (mean: -2.3±2.63 ‰). The correlation between $\delta^{13}C$ and $\delta^{18}O$ values is absent (r = -0.07).

With respect to $\delta^{13}C$, the highest values correspond to the laminated wackestone-packstone (Lw-pl), with a mean of 0.52±1.62‰ (Table II). The remaining facies have negative $\delta^{13}C$ values, being the lowest values those of the nodular limestones

Facies	n	$\delta^{13}C$ (aver±s)	$\delta^{18}O$ (aver±s)	Coef correl (r)
Lwb	1	-2.9	-5.92	
Lwn	2	-5.13±1.63	-6.80±0.21	1
Lw-pl	7	0.52±1.62	-5.07±1.09	-0.19
Lwm	10	-2.13±2.69	-5.48±1.53	-0.03
Lmq	2	-3.79±2.96	-7.31±0.09	1
Lm-wl	3	-4.55±1.21	-4.88±1.31	-0.45
MD	5	-3.59±1.27	-1.27±0.47	0.88

Table II.- Average $\delta^{13}C$ and $\delta^{18}O$ values of facies and correlation coefficient.
Tabla. II.- Promedio de los valores de $\delta^{13}C$ y $\delta^{18}O$ de las facies y coeficiente de correlación.

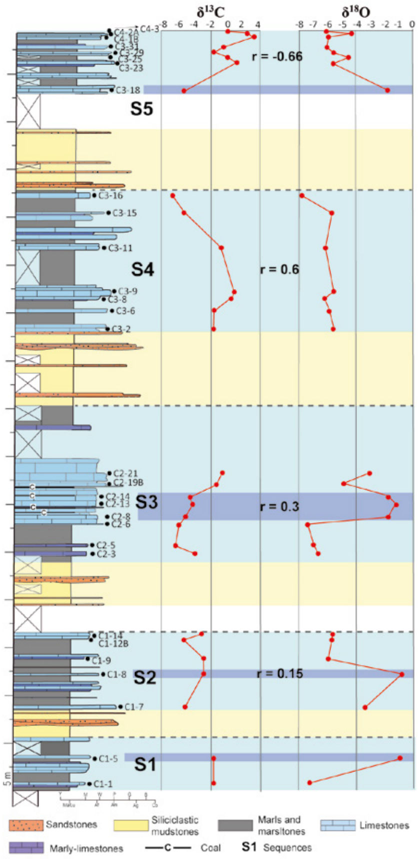

Fig. 2.- Stratigraphic log from Cucho section showing different lithologies and samples. The vertical evolution of $\delta^{13}C$ and $\delta^{18}O$ values. The purple bands correspond to samples with predominant dolomite. In the sequences are indicate the correlation coefficient (r). See the color figure in the Web.
Fig. 2.- Columna estratigráfica de la sección de Cucho presentando las diferentes litologías y muestras. Evolución vertical de los valores de $\delta^{13}C$ y $\delta^{18}O$. Las bandas moradas se corresponden con muestras donde predomina la dolomita. En cada secuencia está indicado el coeficiente de correlación (r). Ver figura en color en la Web.

(Lwn, mean: -5.13±1.63‰). Regarding $\delta^{18}O$, the highest values correspond to samples with dominant dolomite (-1.27±0.47 ‰). The lowest values are those of the massive limestones containing quartz grains (Lmq; mean: -7.31±0.09‰) and the nodular limestones (Lwn; mean -6.80±0.21‰).

The vertical evolution of $\delta^{13}C$ and $\delta^{18}O$ of the sequences present both increasing and decreasing trends (Fig. 2). The correlation coefficients are low, positive and negative. It is remarkable the negative value in S5 (r= -0.66; N=8).

Discussion

The isotopic composition of facies

The negative $\delta^{13}C$ values are consistent with an environment that received variable CO_2 derived from vegetated areas around and in the lake (Talbot and Kelts, 1990). The varying $\delta^{13}C$ can be interpreted in terms of changes in the amount of vegetation development and intensity of the associated pedogenic processes. In this regard, the low $\delta^{13}C$ values of facies Lwn are consistent with intense pedogenesis (Alonso-Zarza and Wright, 2010).

In contrast, high and positive $\delta^{13}C$ values could be related to ^{12}C sequestration from the Total Dissolved Inorganic Carbon (TDIC) in anoxic bottom waters due to water stratification (cf., Leng and Marshall, 2004). This situation would be compatible with a high productivity in the lake, favouring the formation of laminated facies consisting of bioclasts (facies Lw-pl). Whether the high $\delta^{13}C$ values could be a consequence of other processes (e.g, methanogenesis) requires further investigation.

The $\delta^{18}O$ values of the calcite-dominated facies fall within the range of freshwater lakes with no significant effects of evaporative processes, varying slightly due to diagenetic modifications in palustrine areas (Alonso-Zarza and Wright, 2010; Moreau et al., 2023). The low $\delta^{18}O$ values of facies Lmq are consistent with water renewal supplying fine sediment, and the low values of facies Lwn fit ^{16}O-rich surface water in palustrine conditions.

As per the dolomite-bearing samples, with the highest $\delta^{18}O$ values, the small crystal size (i.e., dolomicrite) made it difficult to establish whether dolomite is primary or diagenetic. However, the presence of limestone and marl beds with gypsum pseudomorphs above and below the dolomitic layers suggests dolomite precipitation during very early diagenesis (Arenas et al., 1997) and primary precipitation is not excluded. In either case, high $\delta^{18}O$ values of the dolomite-rich beds are consistent with stages of high salinity and evaporative conditions (Valero-Garcés et al., 2020).

Deepening-shallowing cycles

The isotopic record of the 5 sedimentary cycles in Figure 2 can also be interpreted in terms of changes in environmental conditions, though the small number and sparse distribution of data limits conclusive insights, in particular in S1.

Considering the aforementioned interpretations, the isotopic trends reflect changes in the biogenic CO_2 input, water residence time or evaporation effects, as well as in water supply or water table fluctuations through time (cf. Platt, 1989; Arenas et al., 1997).

Sequence S2 represents deepening with slightly changing biogenic CO_2 inputs trough time. Sequence S3 reflects shallowing, including evaporative conditions, and overall decrease in vegetation cover, likely due to lowering Precipitation/Evaporation rate (P/E).

Sequences S4 and S5 show overall deepening trends, suggestive of rising P/E. But their $\delta^{13}C$ trends are opposite. S4 records a gradual decrease, which is consistent with high organic production from plants. In contrast, S5 shows a complex, overall increasing $\delta^{13}C$ trend, suggesting relatively high TDIC, which might be related to ^{12}C removal from the system in the anoxic bottom during water stratification (Leng and Marshall, 2004). Moreover, the negative correlation coefficient between $\delta^{13}C$ and $\delta^{18}O$ (r=-0.66; N=8) might reflect open lake conditions.

Conclusions

This study presents preliminary insights on the depositional, climatic and hydrological conditions of a lacustrine and palustrine succession in the Miranda-Treviño Basin, based on the stable isotope composition ($\delta^{13}C$ and $\delta^{18}O$), coupled with facies analysis. The sedimentological features of the different sedimentary facies are consistent with the $\delta^{13}C$ and $\delta^{18}O$ values. They reflect changes in depositional, climatic and hydrological conditions: biogenic CO_2 input, water residence time or evaporation effects, water supply and water table fluctuations through time.

Based on the isotopic composition, the studied section reflects a complex evolution that matches that inferred from facies analysis. It consists of several deepening and shallowing cycles, including intense evaporative processes, and varying development of the vegetation cover. The final trend towards deepening and more stable water table coincides with the development of laminated limestones and is parallel to the retrogradation of the fluvial system from the base of S4 onwards. These interpretations should be taken with caution, as more data are required to achieve robust conclusions.

Author contributions

All the authors have participated in the field work, in the interpretation of the geochemical data and in the preparation of the manuscript.

Acknowledgments

Research developed thanks to a pre-doctoral research grant from the University of the Basque Country UPV/EHU. This is also a contribution to the Consolidated Research Group IT-1602-22 of the Basque Government University Research System. We are grateful to two anonymous reviewers for their helpful comments.

References

Alonso-Zarza, A.M., and Wright, V.P. (2010). *Palustrine Carbonates* (A.M Alonso-Zarza and L.H. Tanner, Eds.). Elsevier, Oxford, 103-131. https://doi.org/10.1016/S0070-4571(09)06102-0

Alonso-Zarza, A.M., Calvo, J.P., and Cura, M.A. (1992). *Sedimentary Geology,* 76, 43-61. https://doi.org/10.1016/0037-0738(92)90138-H

Arenas, C., Casanova, J. and Pardo, G., (1997). *Palaeogeography, Palaeoclimatology, Palaeoecology*, 128, 133-155. https://doi.org/10.1016/S0031-0182(96)00052-1

Armenteros, I., Corrochano, I., Alonso-Gavilán, G., Carballeira, J. and Rodríguez, J.M., (2002). In: The Geology of Spain (W. Gibbons and M.T. Moreno, Eds.). The Geological Society, London, 309-315.

Benavente, C., Mancuso, A. and Bohacs, K.M. (2019). Journal of South American Earth Sciences, 95, 102292. https://doi.org/10.1016/j.jsames.2019.102292

Larena, Z., Arenas, C., Baceta, J.I. and Murelaga, X. (2024). Geogaceta, 75, 7-10. https://doi.org/10.55407/geogaceta100686

Leng, M.J. and Marshall, J.D. (2004). Quaternary Science Reviews, 23, 811–831. https://doi.org/10.1016/j.quascirev.2003.06.012

Luzón, A., González, A., Muñoz, A. and Sánchez-Valverde, B. (2002). Journal of Paleolimnology, 28, 441-456. https://doi.org/10.1023/A:1021675227754

Moreau, K., Andrieu, S., Briais, J., Brigaud, B. and Ader, M. (2023). The Depositional Record, 1-35

Riba, O. (1956). La Cuenca Terciaria de Miranda Treviño. Informe inédito. CIEPSA, 28 p.

Riba, O. (1961). Nuevas observaciones sobre el Terciario continental de la Cuenca de Miranda Treviño. Informe inédito. CIEPSA, 19 p.

Riba, O. and Jurado M.J. (1992). Acta Geológica Hispánica 27 (1-2), 177-193.

Talbot, MR. and Kelts, K. (1990). In: Lacustrine Basin Exploration – Case Studies and Modern Analogs (Katz, B.J., Ed.). American Association of Petroleum Geologists, Mem. 50, 99 –112.

Platt, N. H. (1989). Sedimentology, 36, 665-684. https://doi.org/dk8jcf

Valero-Garcés, B.L., Delgado-Huertas, A., Navas, A., Machín, J., González-Sampériz, P. and Kelts, K. (2000) Sedimentology, 47, 1135–1156. https://doi.org/fmqzcs